



## TDDB Reliability Improvement of Cu Damascene with a Bilayer-Structured $\alpha$ -SiC:H Dielectric Barrier

Chiu-Chih Chiang,<sup>a,z</sup> Mao-Chieh Chen,<sup>a,\*</sup> Zhen-Cheng Wu,<sup>b</sup> Lain-Jong Li,<sup>b</sup> Syun-Ming Jang,<sup>b</sup> Chen-Hua Yu,<sup>b</sup> and Mong-Song Liang<sup>b</sup>

<sup>a</sup>Department of Electronics Engineering, National Chiao-Tung University, Hsinchu 300, Taiwan

<sup>b</sup>Taiwan Semiconductor Manufacturing Company, Science-Based Industrial Park, Hsinchu, Taiwan

This work investigates the thermal stability and physical and barrier characteristics of two species of amorphous silicon carbide dielectric films: the nitrogen-containing  $\alpha$ -SiCN film with a dielectric constant of 4.9 and the nitrogen-free  $\alpha$ -SiC film with a dielectric constant of 3.8. The time-dependent-dielectric-breakdown (TDDB) lifetime of the Cu damascene metallization structure is greatly improved by using an  $\alpha$ -SiCN/ $\alpha$ -SiC bilayer dielectric stack as the barrier layer. This improvement is attributed to the lower leakage current of  $\alpha$ -SiC, absence of nitridation on the Cu surface, and better adhesion of  $\alpha$ -SiC on Cu and organosilicate glass intermetal dielectric. Although the  $\alpha$ -SiC film has a very low deposition rate, the  $\alpha$ -SiCN/ $\alpha$ -SiC bilayer dielectric is a favorable combination for the barrier layer because  $\alpha$ -SiCN can protect  $\alpha$ -SiC from plasma attack, such as O<sub>2</sub> plasma attack during photoresist stripping and organosilicate plasma attack during organosilicate glass deposition.

© 2004 The Electrochemical Society. [DOI: 10.1149/1.1637358] All rights reserved.

Manuscript submitted October 15, 2002; revised manuscript received August 11, 2003. Available electronically January 8, 2004.

As the device dimensions continuously shrink, the operation speed of the integrated circuits is dominated by the resistance-capacitance (RC) time constant of the interconnect system. In order to minimize signal propagation delay, it is inevitable to use low-dielectric-constant (low- $k$ ) materials as the inter- and intralayer dielectrics (ILD). While many low- $k$  ( $k < 3$ ) materials have been used as ILDs, silicon nitride with a high dielectric constant ( $k > 7$ ) is still the primary candidate for the barrier required in copper damascene structures. Thus, it is desirable to replace silicon nitride by other new materials with a lower  $k$ -value to further reduce the effective dielectric constant of the Cu interconnect system. In recent years, increasing interest has been focused on the study of low stress and thermally stable low- $k$  amorphous silicon carbide-based ( $\alpha$ -SiC:H) films deposited by plasma-enhanced chemical vapor deposition (PECVD) using organosilicate gases (OSGs).<sup>1-5</sup> In this work, we first investigate the thermal stability and physical and barrier characteristics of two species of  $\alpha$ -SiC:H low- $k$  dielectric films ( $k < 5$ ). This is followed by investigating the TDDB lifetime of a Cu damascene metallization structure having a bilayer dielectric barrier made up of these two species of films.

### Experimental

Two species of PECVD amorphous silicon carbide with  $k$ -values less than 5 are investigated with respect to the thermal stability and physical and barrier characteristics. The silicon carbide films of  $\alpha$ -SiCN and  $\alpha$ -SiC, designated as SCN and SC, respectively, were deposited on p-type, (100)-oriented Si wafers to a thickness of 50 nm. In addition, an SCN/SC bilayer dielectric film, designated as SCB, was also prepared with a 5 nm SC film deposited on the Si substrate followed by a 45 nm SCN film deposited on top of it. A metal electrode (Cu or Al) was deposited on the silicon carbide films to construct the metal-insulator-semiconductor (MIS) capacitor structure. For the Cu-electrode MIS capacitors, a Cu layer of 200 nm thickness was sputter deposited on the silicon carbide films, followed by a reactive sputter deposition of a 50 nm thick TaN layer on the Cu surface for the purpose of preventing oxidation of the Cu electrode during the subsequent thermal process. Al electrode samples were also prepared by depositing 500 nm thick Al layers directly on the silicon carbide dielectric surfaces. For better electrical measurements, a 500 nm thick Al layer was also deposited on the back side of the Si substrate for all samples. The TaN/Cu-electrode MIS capacitors were then annealed at 400°C for 30 min in an N<sub>2</sub> ambient. This annealing step eliminates the plasma-induced damage

during the sputter deposition of TaN/Cu-electrodes and also provides the driving force for Cu diffusion. Cu damascene structures were constructed for the TDDB reliability study. Figure 1 shows the comb 1/serpentine/comb 2 test structure and the cross-sectional transmission electron microscopy (TEM) micrograph of the Cu damascene structure employed in this study. A PECVD OSG ( $\alpha$ -SiOC:H) film was first deposited to serve as the intermetal dielectric (IMD). After patterning of 0.20/0.20  $\mu$ m linewidth/space trenches in the OSG dielectric, the damascene Cu features were electrochemically deposited on a 30 nm thick TaN liner barrier. Following the Cu chemical mechanical polish, either an SCN (50 nm) single-layer dielectric or an SCN (45 nm)/SC (5 nm) bilayer dielectric stack (with the thin SC layer deposited first on the Cu/OSG surface), which is designated as SCB, was prepared as the barrier. The Cu damascene structure with an SC single-layer barrier was not used in this study because the SC dielectric has a very low deposition rate

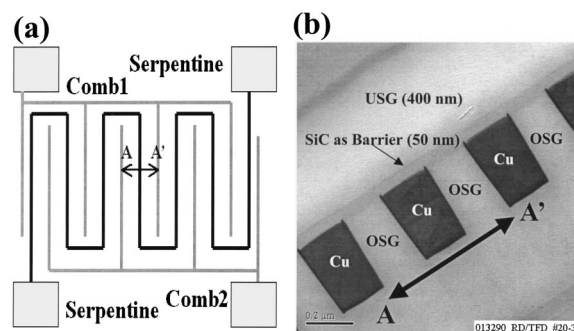


Figure 1. (a) Schematic diagram of comb 1/serpentine/comb 2 test structure and (b) cross-sectional TEM micrograph of the Cu damascene structure.

Table I. Some basic data of  $\alpha$ -SiC:H dielectrics.

| Sample                       | SCN                                     | SC                          |
|------------------------------|---|-----------------------------|
| Structure                    | $\alpha$ -SiCN                          | $\alpha$ -SiC               |
| Deposition gas               | $\text{SiH}(\text{CH}_3)_3/\text{NH}_3$ | $\text{SiH}(\text{CH}_3)_3$ |
| Deposition temperature (°C)  | 350                                     | 350                         |
| Deposition rate (nm/min)     | 176                                     | 2.6                         |
| Refractive index (at 633 nm) | 1.90                                    | 1.85                        |
| Dielectric constant at 1 MHz | 4.9                                     | 3.8                         |

\* Electrochemical Society Active Member.

<sup>z</sup> E-mail: ccchiang.ee88g@nctu.edu.tw

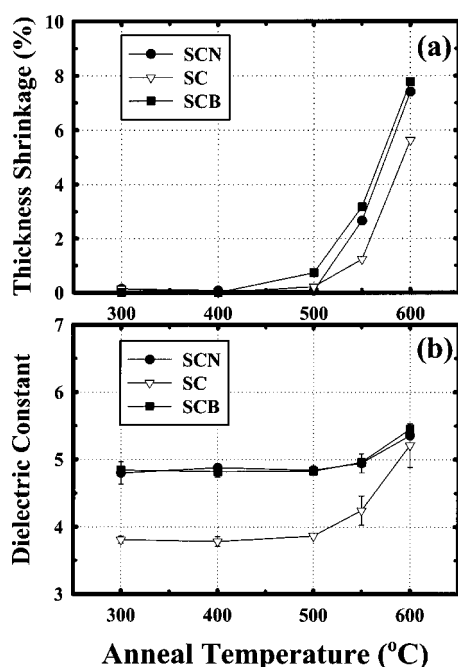


Figure 2. (a) Thickness shrinkage and (b) dielectric constant vs. annealing temperature for three samples of PECVD  $\alpha$ -SiC:H dielectrics.

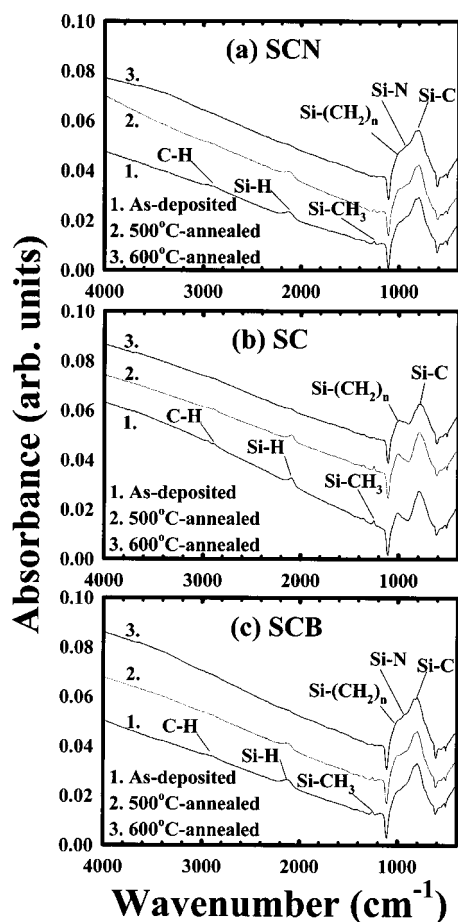


Figure 3. FTIR spectra for three samples of PECVD  $\alpha$ -SiC:H dielectrics (a) SCN, (b) SC, and (c) SCB.

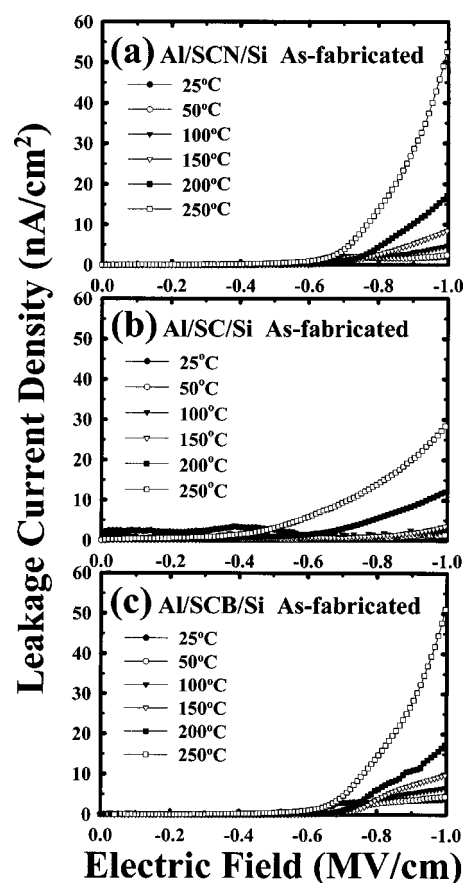


Figure 4. Current density vs. electric field, measured at various temperatures, for (a) Al/SCN/Si, (b) Al/SC/Si, and (c) Al/SCB/Si MIS capacitors.

and is susceptible to plasma damage. Finally, the Cu damascene structure was passivated with an undoped silicate glass capping layer of 400 nm thickness.

An HP4145B semiconductor parameter analyzer was used to measure the dielectric leakage current and provide bias for the bias-temperature-stress (BTS) test. The dielectric film thickness and refractive index were measured using an N&K analyzer at 633 nm wavelength. Fourier transform infrared spectroscopy (FTIR) was used to analyze the chemical bonding of the dielectrics. The adhesion of films was measured using a four-point bending technique.<sup>6</sup> X-ray photoelectron spectroscopy (XPS) was used to analyze the elemental composition of the Cu surface. The  $k$ -value of the dielectrics was determined by the maximum capacitance of the Al-gated MIS capacitors measured at 1 MHz using a Keithley Package 82 system.

### Results and Discussion

Table I shows the deposition gas, deposition temperature, deposition rate, and the refractive index and dielectric constant for the two species of PECVD amorphous silicon carbide investigated in this work. Notably, the deposition rate of SC, which contains no nitrogen at all, is much slower than that of SCN. Figure 2 shows the film thickness shrinkage as well as dielectric constant as a function of annealing temperature (for 30 min in an  $N_2$  ambient) for the SCN, SC, and SCB films. The SC film has a dielectric constant of about 3.8, while the nitrogen-containing SCN film has a higher dielectric constant of about 4.9, presumably due to the polarization contribution from nitrogen. Moreover, higher carbon content would lead to a decrease in electronic and ionic polarizations, resulting in a lower  $k$ -value of films.<sup>7,8</sup> The effective dielectric constant of the SCB film, which is a bilayer SCN (45 nm)/SC (5 nm) film, should be very

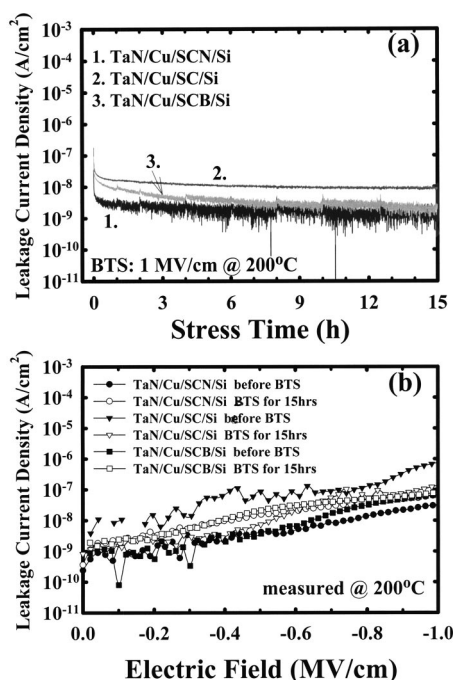
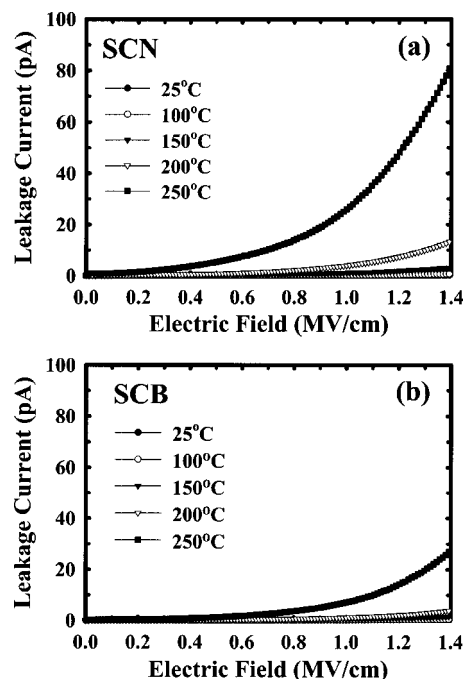


**Figure 5.** (a) Current transient during BTS (1 MV/cm at 200°C) and (b) instantaneous current density vs. electric field before and after the BTS for the TaN/Cu/SCN/Si, TaN/Cu/SC/Si, and TaN/Cu/SCB/Si MIS capacitors.

close to that of the SCN film. The substantial increase in thickness shrinkage and dielectric constant at temperatures above 500°C is attributed to the outgassing of the methyl group, resulting in a decrease and eventual disappearance of Si-CH<sub>3</sub>, C-H, and Si-H peak heights, as shown in the FTIR spectra illustrated in Fig. 3.

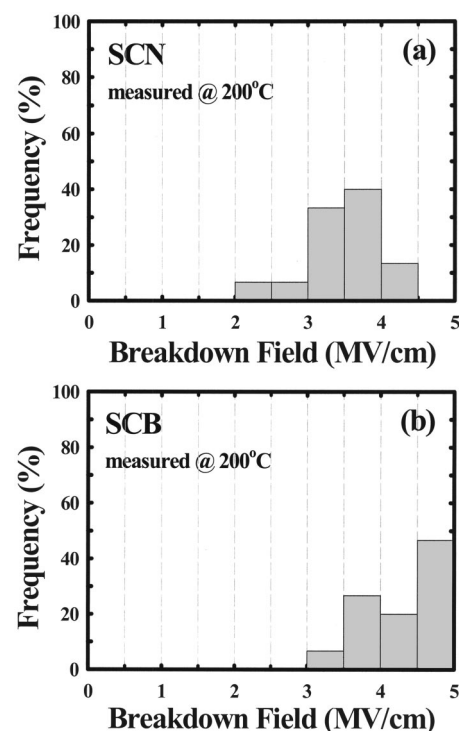
The leakage current density of the Al/SCN/Si, Al/SC/Si, and Al/SCB/Si MIS capacitors measured at various temperatures is illustrated in Fig. 4. The TDDB was measured on the TaN/Cu-electrode SCN (50 nm), SC (50 nm), and SCB (45 nm SCN/5 nm SC) MIS samples at 200°C under a bias stress of 1 MV/cm. Figure 5 illustrates the leakage current transient during the BTS and the instantaneous leakage current density vs. applied electric field (in accumulation mode) before and after the BTS. All the samples remained stable under the BTS up to at least 15 h. This implies that both SCN and SC dielectric bulk films were capable of preventing Cu permeation.

Figure 6 and 7 illustrate the results of leakage current measurements and breakdown field statistics, respectively, for the Cu damascene metallization structures with a barrier layer of SCN (50 nm) as well as SCB (45 nm SCN/5 nm SC). The breakdown field is defined as the field strength such that the leakage current between comb 1/comb 2 (grounded) and serpentine (positive biased) exceeds 1 mA, and the histogram of the breakdown field was constructed from the data obtained by measuring 29 samples. The Cu damascene structure with an SCB bilayer barrier exhibits a much lower leakage current and higher breakdown field than that with an SCN single-layer barrier. Figure 8 shows the TDDB measurement at 200°C under a bias stress of 2 MV/cm for the Cu damascene structure with different barrier of SCN and SCB layer, and Fig. 9 shows the measured time-to-breakdown vs. BTS stress field. The damascene structure with an SCB bilayer barrier has a higher value of TDDB lifetime than the structure using an SCN single-layer barrier of the same thickness. All these observations are attributed to the lower leakage current of SC dielectric film (Fig. 4), because both dielectric films were capable of preventing Cu permeation (Fig. 5). In addition, the adhesion strength of SC/Cu and SC/OSG interfaces is superior to that of SCN/Cu and SCN/OSG interfaces, as shown in Table II. XPS analysis shows that there is a nitridation layer of CuN<sub>x</sub> at the



**Figure 6.** Leakage current vs. electric field, measured at various temperatures, for Cu damascene metallization structure with a barrier layer of (a) SCN and (b) SCB.

SCN/Cu interface but not at the SC/Cu interface (not shown). The ionized Cu atoms of CuN<sub>x</sub> compound have a lower activation energy for diffusion,<sup>9</sup> leading to the degradation of the TDDB reliability of Cu damascene structure with an SCN single-layer barrier. Because the SC dielectric has a very low deposition rate, we believe that the SCN/SC bilayer dielectric is a favorable combination for the barrier



**Figure 7.** Histogram of breakdown field for the Cu damascene metallization structure with a barrier layer of (a) SCN and (b) SCB.

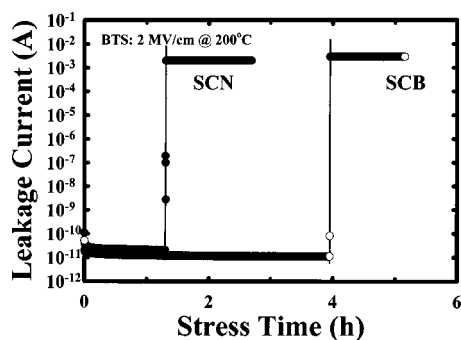


**Figure 8.** Current transient during BTS (2 MV/cm at 200°C) for Cu damascene structure with a barrier layer of SCN and SCB.

because the nitrogen-containing SCN film with the  $\text{SiN}_x$  compound can protect the SC film from plasma attack, such as  $\text{O}_2$  plasma attack during photoresist stripping<sup>10</sup> and organosilicate plasma attack during OSG deposition.

### Conclusion

The TDDDB lifetime of Cu damascene metallization structure is greatly improved by using an  $\alpha$ -SiCN/ $\alpha$ -SiC bilayer dielectric stack

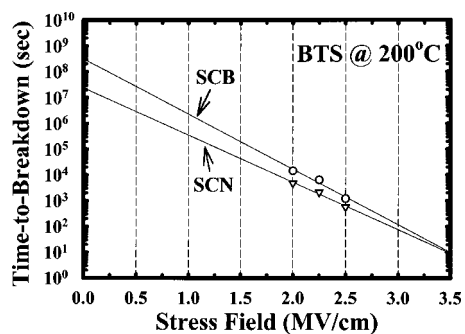


**Figure 9.** Time-to-breakdown vs. BTS stress fields at 200°C for Cu damascene structure with a barrier layer of SCN and SCB.

**Table II.** Adhesion strength of  $\alpha$ -SiC:H dielectric/Cu and  $\alpha$ -SiC:H dielectric/OSG interfaces.

| Film scheme          | Adhesion Gc (J/m <sup>2</sup> ) |
|----------------------|---------------------------------|
| SCN/Cu/TaN/PE-OX/Si  | 2.76                            |
| SC/Cu/TaN/PE-OX/Si   | 8.44                            |
| SCN/OSG/SiN/PE-OX/Si | 4.44                            |
| SC/OSG/SiN/PE-OX/Si  | 9.34                            |

as the barrier layer. This improvement is attributed to the lower leakage current of  $\alpha$ -SiC, absence of nitridation on Cu surface, and better adhesion of  $\alpha$ -SiC on Cu and OSG IMD. Although the  $\alpha$ -SiC film has a very low deposition rate, the  $\alpha$ -SiCN/ $\alpha$ -SiC bilayer dielectric is a favorable combination for the barrier layer because  $\alpha$ -SiCN can protect  $\alpha$ -SiC from plasma attack, such as  $\text{O}_2$  plasma attack during photoresist stripping and organosilicate plasma attack during OSG deposition.

### Acknowledgment

The authors give their gratitude to C. H. Yao and B. T. Chen of TSMC, and S. Y. Chang of NTHU for their valuable technical support.

*The National Chiao-Tung University assisted in meeting the publication costs of this article.*

### References

1. M. J. Loboda, J. A. Seifferly, and F. C. Dall, *J. Vac. Sci. Technol. A*, **12**, 90 (1994).
2. M. J. Loboda, J. A. Seifferly, C. M. Grove, and R. F. Schneider, *Mater. Res. Soc. Symp. Proc.*, **447**, 145 (1997).
3. P. Xu, K. Huang, A. Patel, S. Rathi, B. Tang, J. Ferguson, J. Huang, C. Ngai, and M. Loboda, in *Proceedings of IEEE 1999 IITC*, p. 109 (1999).
4. M. J. Loboda, *Microelectron. Eng.*, **50**, 15 (2000).
5. S. G. Lee, Y. J. Kim, S. P. Lee, H. S. Oh, S. J. Lee, M. Kim, I. G. Kim, J. H. Kim, H. J. Shin, J. G. Hong, H. D. Lee, and H. K. Kang, *Jpn. J. Appl. Phys., Part 1*, **40**, 2663 (2001).
6. T. Scherban, B. Sun, J. Blaine, C. Block, B. Jin, and E. Andideh, in *Proceedings of IEEE 2001 IITC*, p. 257 (2001).
7. B. K. Hwang, M. J. Loboda, G. A. Cerry, R. F. Schneider, J. A. Seifferly, and T. Washer, in *Proceedings of IEEE 2000 IITC*, p. 52 (2000).
8. J. Y. Kim, M. S. Hwang, Y. H. Kim, H. J. Kim, and Y. Lee, *J. Appl. Phys.*, **90**, 2469 (2001).
9. J. D. McBrayer, R. M. Swanson, and T. W. Sigmon, *J. Electrochem. Soc.*, **133**, 1242 (1986).
10. P. T. Liu, T. C. Chang, H. Su, Y. S. Mor, Y. L. Yang, H. Chung, J. Hou, and S. M. Sze, *J. Electrochem. Soc.*, **148**, F30 (2001).